Table I. Comparison of the Efficiency Parameter (Percent) for 3 to 9 Pure Aluminum at $T = 450$ °C and $\varepsilon = 0.3$

Test Data[4]		Efficiency Parameter, η (Pct)	
Strain Rate $\dot{\varepsilon}$ (S^{-1})	Flow Stress σ (Mpa)	Method of Ref. 4 Eq. [6]	Present Study Eq. [7]
0.001	5.9	35.05	35.05
0.01	9.8	38.20	36.73
0.1	16.5	30.93	35.26
1.0	23.3	27.67	26.40
10.0	34.8	25.65	28.80
100.0	44.0	14.69	17.48

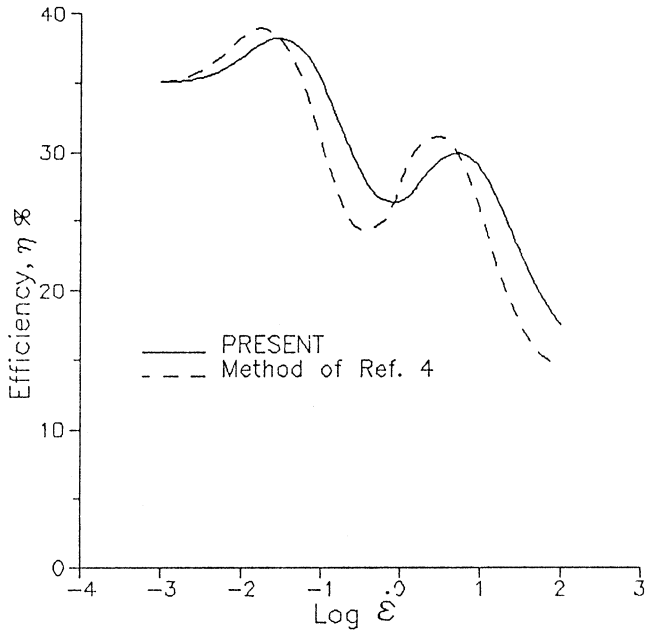

Fig. 1—Efficiency parameter (η) with the strain rate ($\dot{\varepsilon}$) from the data of Table I.

rates. This is mainly due to the erroneous assumption of power law holding good from zero to each strain rate. In the present study, the continuous piecewise polynomial is fitted for σ-$\dot{\varepsilon}$ data; and σ is obtained from this curve at any $\dot{\varepsilon}$, as required in the evaluation of the integral in Eq. [7], which is obviously more efficient.

REFERENCES

1. Y.V.R.K. Prasad, H.L. Gegel, S.M. Doraivelu, J.C. Malas, J.T. Morgan, K.A. Lark, and D.R. Barker: *Metall. Trans. A*, 1984, vol. 15A, pp. 1883-92.
2. H.L. Gegel, J.C. Malas, S.M. Doraivelu, and V.A. Shende: *Metals Handbook*, ASM, Metals Park, OH, 1987, vol. 14, pp. 417-38.
3. J.M. Alexander: in *Modelling of Hot Deformation of Steels*, J.G. Lenard, ed., Springer-Verlag, Berlin, 1989, pp. 101-15.
4. N. Ravichandran and Y.V.R.K. Prasad: *Metall. Trans. A*, 1991, vol. 22A, pp. 2339-48.

Computational Modeling of NbC/Laves Formation In INCONEL 718 Equiaxed Castings

L. NASTAC and D.M. STEFANESCU

The importance of modeling of NbC/Laves formation in INCONEL* 718 is broadly discussed in the literature.[1–8] It is also known that the distribution of carbides, Laves phases, and microporosities in alloy 718 is affected by the solidification path. The volume fraction of solid is a function of local growth velocity, solidification time, solidus temperature, local temperature gradient, *etc.* The redistribution of elements strongly affects the phase evolution in common superalloys which, in turn, affects their mechanical properties and stability at elevated temperature.

*INCONEL is a trademark of INCO Alloys International, Inc., Huntington, WV.

The goal of this work is to develop a solidification kinetics model for prediction of NbC and Laves phase evolution during casting solidification. Previous studies on alloy 718 showed that both NbC and Laves produce intergranular liquid films due to the intergranular distribution of Nb and C.[5,6] Also, the ability of Laves to promote intergranular liquation cracking (microfissuring and hot cracking) during heat treatment is much higher than that of NbC. This is because the temperature of Laves phase formation is usually lower than that of NbC, *i.e.*, liquation initiates at the eutectic-Laves temperature.

Experimental evidence demonstrates that the amount of NbC and Laves in cast alloy 718 is different from that predicted by phase equilibrium. The reason for this difference is that while in equilibrium processes mass diffusion transport is very fast compared with solidification kinetics ($V << D/L$), in casting processes, solidification kinetics is much closer to diffusivity ($V <= D/L$). Thus, solidification kinetics cannot be ignored.

In References 5 and 6, it was demonstrated that the carbon content of alloy 718 directly affects the volume fraction of carbides. This is readily explained from a pseudoternary (γ-NbC-Laves) phase diagram.[5] A schematic of an isothermal section through the space diagram of the pseudoternary γ-NbC-Laves system, just above the ternary eutectic, is presented in Figure 1.

The as-cast alloy could contain a higher volume fraction of NbC and Laves phase than what the phase diagram suggests due to the microsegregation during solidification. The relative volume fractions of NbC and Laves depend on the C/Nb ratio. Alloys with high C/Nb ratio will have a higher volume fraction of carbide than alloys with low C/Nb ratio. The possible solidification paths of the γ-NbC-Laves, schematically presented in Figure 1, are summarized in Table I.

L. NASTAC, formerly Graduate Research Assistant, Department of Metallurgical and Materials Engineering, The University of Alabama, is Senior Engineer with Concurrent Technologies Corporation, Johnstown, PA 15904. D.M. STEFANESCU, University Research Professor and Director of the Solidification Laboratory, is with the Department of Metallurgical and Materials Engineering, The University of Alabama, Tuscaloosa, AL 35487.

Manuscript submitted December 27, 1996.

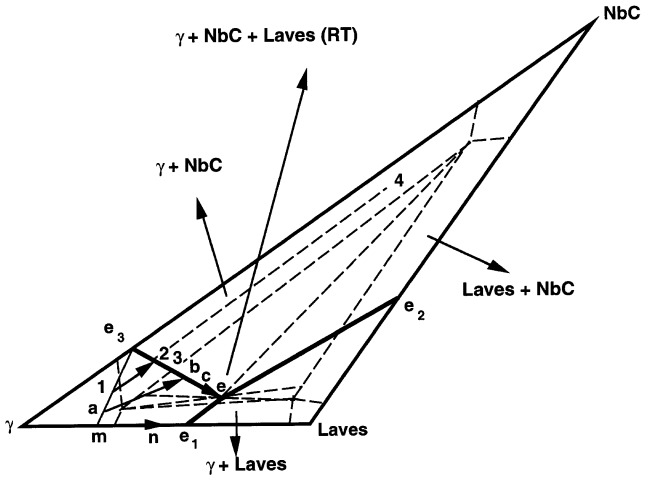

Fig. 1—Schematic representation of solidification paths based on isothermal section through the space diagram at the pseudoternary eutectic temperature.

Table I. Summary of Possible Solidification Outcome of γ-NbC-Laves System as a Function of the C/Nb Ratio

		Microstructure	
C/Nb Ratio	Solidification Path	Laves	NbC
Sufficiently high	1-2-4	no	maximum
High	1-2-3	low	high
Sufficiently low	m-n-e_1	maximum	no
Medium (alloy 718)	a-b-c-e	medium	medium

The proposed model is based on the following assumptions: instantaneous nucleation of carbides, carbide growth only in the liquid, negligible interference between growing carbides, carbides pushed by the solid/liquid (S/L) interface,[9] volume diffusion limited growth of carbides, and binary diffusion couple.

The following calculations are required to predict the NbC/Laves phase formation in INCONEL 718: (1) coupling of macrotransport—solidification kinetics models, (2) equiaxed dendritic growth of the γ phase, (3) nucleation and growth of NbC assuming that the slow step is the volume diffusion of carbon from the liquid to the NbC/Laves interface, (4) modeling of the solute redistribution of Nb and C, and (5) growth of the Laves phase. They will be discussed in detail in the following paragraphs.

(1) The macroscopic model for heat transport calculation was a simple one-dimensional, implicit, control volume model. The boundary conditions were selected such as to match the experimental cooling rates obtained in our previous work.[15] The coupling between the macrotransport and the solidification kinetics models is accomplished through the Latent Heat Method,[18] where the heat source term, $\dot{Q}$, is

$$\dot{Q} = \rho_\gamma L_\gamma \frac{\partial f_\gamma}{\partial t} + \rho_{\text{NbC}} L_{\text{NbC}} \frac{\partial f_{\text{NbC}}}{\partial t} + \rho_{\text{Laves}} L_{\text{Laves}} \frac{\partial f_{\text{Laves}}}{\partial t}$$

with

$$f_\gamma + f_{\text{NbC}} + f_{\text{Laves}} = 1 \qquad [1]$$

where f is the fraction of phase, ρ is the density, and L is the latent heat of fusion.

(2) The equiaxed dendritic growth is based on the alloy 718 pseudobinary phase diagram.[1,6] The primary driving force for growth is considered to be the liquid Nb concentration. The model for equiaxed dendritic growth of alloy 718 is described elsewhere.[15,16,17] It is applied here to calculate the evolution of the fraction of solid of the γ phase.

(3) It is assumed that the growth mechanism of NbC is governed by the carbon diffusion from the liquid to the NbC/Laves interface and by the reaction kinetics between Nb and C. Applying the metastable progress variable approach, it can be shown that the chemical reaction rate is very high, *i.e.*, the kinetics of reaction can be neglected in further calculations (Appendix I). Thus, carbon concentration is depleted at the NbC/Laves interface, and the amount of NbC precipitated depends on the volume diffusion of carbon from the liquid to the NbC/Laves interface.

The schematic representation of the diffusion pattern for NbC as well as the main model assumptions are discussed in Appendix II. It is assumed that the carbides nucleate instantaneously at the equilibrium solidification temperature of alloy 718 (T = 1609 K). The solution of volume diffusion-limited growth is described by the averaging method:

$$V_{\text{NbC}} = \frac{\Omega_c}{\phi_{\text{NbC}}} \left(\frac{D_L}{R_D - R_{\text{NbC}}} \right) \qquad [2]$$

with

$$\phi_{\text{NbC}} = \frac{4\pi R_{\text{NbC}}}{A_s} \quad \text{and} \quad R_D = \frac{3}{4\pi} \left(\frac{\nu_L}{N_{\text{NbC}}} \right)^{1/3}$$

where Ω_c is the solutal supersaturation, ϕ_{NbC} is the shape factor of the NbC that accounts for its real geometry, R_D is the radius of the microvolume element, R_{NbC} is the radius of the NbC particle, A_s is the surface area of the blocky-shaped NbC particle, v_L is the volume of liquid, and N_{NbC} is the volumetric density of carbides in the liquid. Experimental measurements in Reference 19 demonstrated that the shape factor of NbC varies between 0.54 and 0.74 and that it decreases with cooling rate.

(4) The redistribution of both C and Nb are calculated with the modified model described in Reference 14. The main assumptions are as follows: solute transport is calculated in both solid and liquid phases assuming Fick's law for binary systems in spherical coordinates; the solid/liquid interface is planar and under local equilibrium; there is no solute flow into or out of the volume element (closed system); and there is constant initial liquid concentration. The overall mass balance is described by

$$\frac{1}{\rho_\gamma \nu_\Omega} \int_{\nu_\Omega} \rho_\gamma C \, d\nu_\Omega = C_0 - \frac{\nu_{\text{NbC}}}{\nu_\Omega} \frac{\rho_{\text{NbC}}}{\rho_\gamma} \text{ pct } C_{\text{NbC}} \qquad [3]$$

with

$$\int_{\nu_\Omega} C \, d\nu_\Omega = \int_0^{R^*} 4\pi r^2 \, C_S \, dr + \int_{R^*}^{R_f} 4\pi r^2 \, C_L \, dr \qquad [4]$$

where C_0 is the initial concentration of the alloy, v_{NbC} is the actual volume of carbides, v_Ω is the volume of the element over which the mass balance is calculated, and pct C_{NbC} is the C concentration in NbC.

The overall mass balance is used to couple the concentration fields in both the solid and liquid phases.

Note that the cross-interdiffusion coefficients, as required in calculation of pseudoternary systems, are usually one

Table II. Data Used in the Calculations

Element	D_S ($m^2\ s^{-1}$)	D_L ($m^2\ s^{-1}$)	ρ ($kg\ m^{-3}$)	k	C_{eut} (Wt Pct)
Nb	1×10^{-12}	1×10^{-9}	8400	0.48	19.1
C	2×10^{-10}	2×10^{-9}	2400	0.2	2.22

Phase	L ($J\ kg^{-1}$)	Γ (K m)	ρ ($kg\ m^{-3}$)	K_L ($W\ m^{-1}\ K^{-1}$)	m_L (K wt pct^{-1})	T_L (°C)	C (Wt Pct)	Nb (Wt Pct)
NbC	435,000	—	7200	—	—	1330.0	15.0	85.0
IN718	295,000	3×10^{-7}	7620	30.0	−10.83	1330.0	0.06	5.25

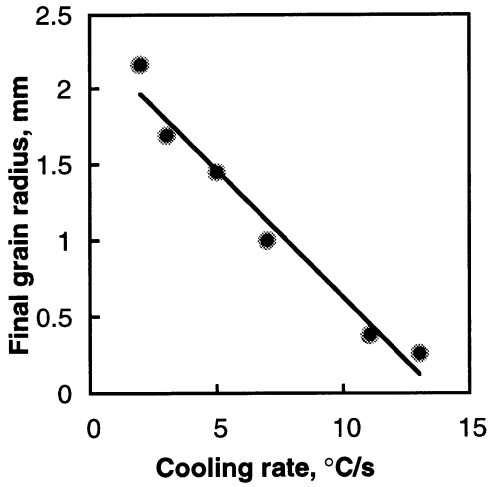

Fig. 2—Measured grain radius *vs* cooling rate.

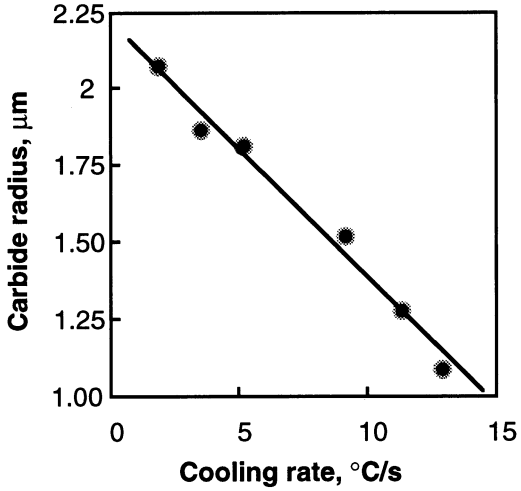

Fig. 3—Measured carbide radius *vs* cooling rate.

order of magnitude lower than normal diffusion coefficients[12,13] and are neglected in this analysis.

The solution of this diffusion couple is a modified version of the Nastac and Stefanescu model[14] and consists of the following equations:

Interface concentration:

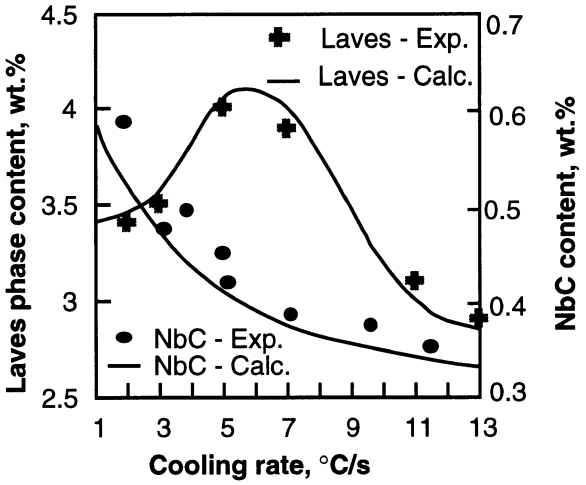

Fig. 4—Experimental and calculated amounts of NbC and Laves phase as a function of cooling rate. Initial carbon and niobium contents were 0.06 and 5.25 wt pct, respectively.

$$C_L^* = \frac{C_0 \left(k\, I_S + I_L - \frac{1}{3} \right) + Q}{k\, I_S + I_L - \frac{1}{3} + \frac{(1-k)\, f_S}{3}} \qquad [5]$$

where $f_S = (R^*/Rf)^3$ and Q, I_S, and I_L are calculated with

$$Q = \frac{\nu_{NbC}}{\nu_\Omega} \frac{\rho_{NbC}}{\rho_\gamma} \text{ pct } C_{NbC}$$

$$I_S = \frac{2 f_S}{\pi^2} \sum_{n=1}^{\infty} \frac{1}{n^2} \exp \left[-\left(\frac{n\,\pi}{f_S^{1/3}} \right)^2 \frac{D_S\, t}{R_f^2} \right]$$

and

$$I_L = 2 f_S^{2/3} (1 - f_S^{1/3}) \sum_{n=1}^{\infty} \frac{1}{\alpha_n^2} \exp \left[-\left(\frac{\alpha_n}{1 - f_S^{1/3}} \right)^2 \frac{D_L\, t}{R_f^2} \right]$$

$$\text{with} \quad \tan \alpha_n = \frac{R_f\, \alpha_n}{R_f - R^*} \qquad [6]$$

The average concentration in the liquid phase is

$$\langle C_L \rangle^L = \frac{4\,\pi}{V_L} \int_{R^*}^{R_f} r^2\, C_L(r)\, dr = C_L^* + 6$$
$$(C_0 - C_L^*)\, R^{*2}\, \frac{R_f - R^*}{R_f^3 - R^{*3}} \sum_{n=1}^{\infty} \frac{\exp(-\lambda_n\, D_L\, t)}{\alpha_n^2} \qquad [7]$$

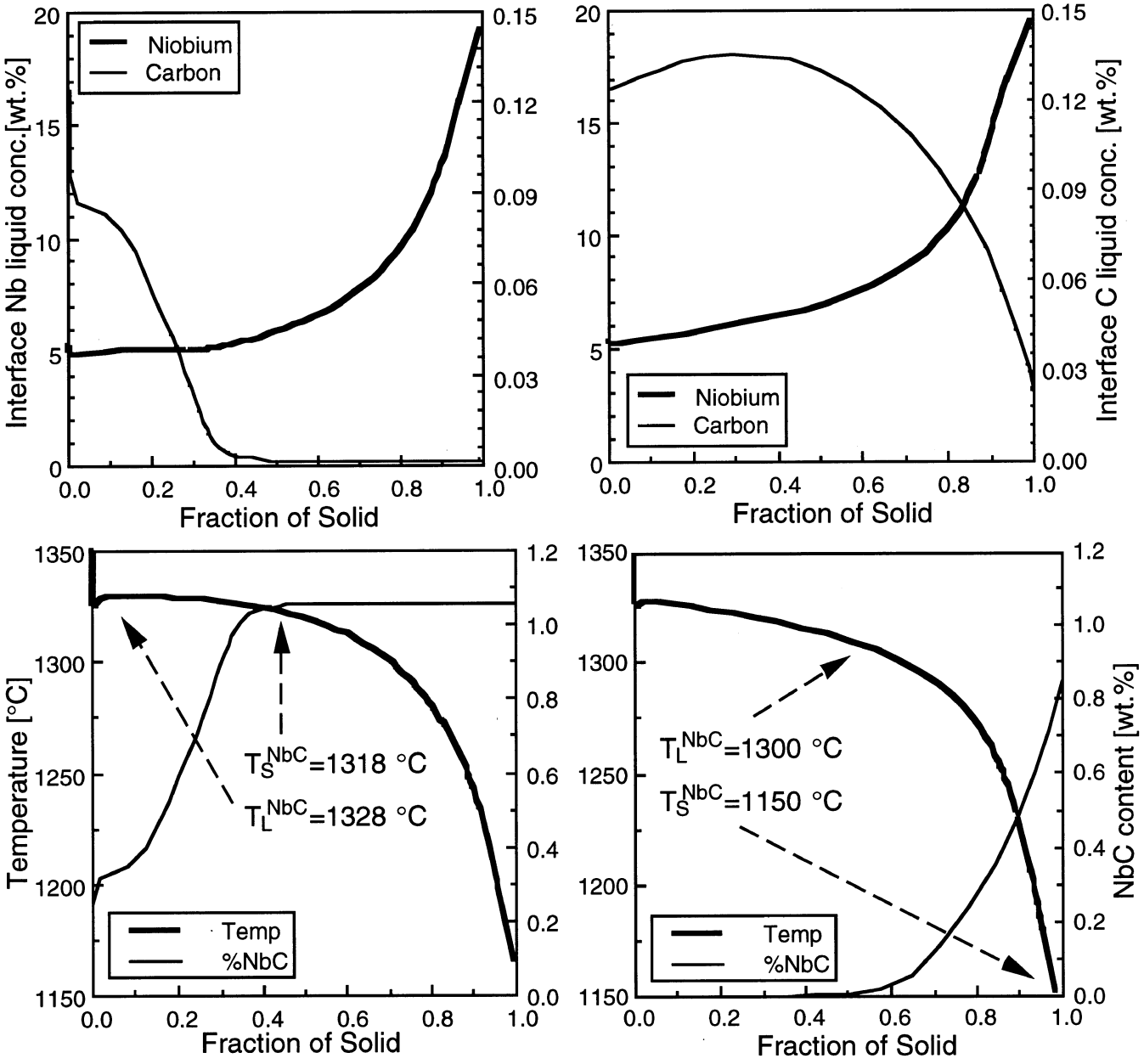

Fig. 5—Influence of cooling rate (left—$\dot{T}$ = 1 K s^{-1}, and right—$\dot{T}$ = 9 K s^{-1}) on the amount of NbC precipitated in as-cast INCONEL 718. Initial carbon and niobium contents were 0.125 and 5.25 wt pct, respectively.

where v_L is the volume of the liquid phase, r is the radial coordinate, C_0 is the initial concentration, the eigenvalue, λ_{nL}, is $\lambda_{nL} = \alpha_n^2(R_f - R^*)^{-2}$, and α_n is the nth root of the equation $\alpha_n R_f \cot \alpha_n = R_f - R^*$.

(5) The Laves phase starts to form when the concentration of Nb reaches the eutectic (γ + Laves) composition, which is 19.1 wt pct Nb. The kinetics of Laves is very high due to its morphology (eutectic or globular-type divorced eutectic) and appearance as discontinuous thin films at the grain boundaries. It is assumed that the amount of Laves phase is directly related to the Nb concentration.[15,16,17]

The physical properties used in the present calculations are shown in Table II. The measured equiaxed grain radius and carbide radius as a function of cooling rate are presented in Figures 2 and 3, respectively. The experimental procedure is described in References 15 and 16. The experimental and calculated amounts of NbC and Laves phase as a function of cooling rate for the initial carbon and niobium contents of 0.06 and 5.25 wt pct, respectively, are shown in Figure 4.

The influence of cooling rate on the amount of NbC precipitated in cast INCONEL 718, when the initial carbon and niobium contents were 0.125 and 5.25 wt pct, respectively, is presented in Figure 5. As the cooling rate increases, the amount of precipitated NbC decreases and falls short of the maximum (equilibrium) amount. Note that the liquidus and solidus temperatures, T_L^{NbC} and T_S^{NbC}, are strongly dependent on the cooling rate.

In this work, a computational model for the prediction of niobium carbides and Laves phase evolution during solidification was developed and validated. It was demonstrated that an optimum combination between C and Nb as

a function of cooling rate has to be achieved to minimize the amount of both NbC and Laves, in order to obtain a Laves-free microstructure. This optimum combination may result in improved mechanical properties, such as good stress-rupture ductility due to the formation of a higher volume fraction of carbides (spherical shape), improved room-temperature tensile strength and ductility due to the elimination of the Laves phase, *etc.*

APPENDIX I
Thermodynamics of NbC

From Reference 10,

$$\text{Nb} + \text{C} \rightarrow \text{NbC},\ \Delta G = -140{,}100 + 11.76\ T\ (^{\circ}\text{C}) \quad \text{(J)} \qquad \text{[Ia]}$$

Then,

$$K_{eq} = \frac{a_{\text{NbC}}}{a_{\text{Nb}}\, a_{\text{C}}} \cong \frac{X_{\text{NbC}}}{X_{\text{Nb}}\, X_{\text{C}}} \frac{1}{\gamma_{\text{Nb}}\, \gamma_{\text{C}}} = \exp\left(-\frac{\Delta G}{\text{R}T}\right) \qquad \text{[Ib]}$$

When $T > 1500$ K, $K_{eq} > 10^4$; *i.e.*, the chemical reaction rate is very high and can be neglected.

APPENDIX II
Growth of spherical precipitates

It is assumed that the spherical growth is only due to the mass diffusion in the liquid phases. The assumed diffusion profile during growth is shown in Figure II.

Fick's law only in the liquid phase gives

$$\frac{\partial C_L}{\partial t} = \frac{1}{r^2} \frac{\partial}{\partial r}\left(r^2\, D_L \frac{\partial C_L}{\partial r}\right) \qquad \text{[IIa]}$$

$$\text{B.Cs.} \qquad C(r = R^*,t) = C_L^* \quad C(r \rightarrow \infty,t) = \langle C \rangle_L \qquad \text{[IIb]}$$

$$\text{I.C.} \qquad C(r,t = 0) = \langle C \rangle_L \quad r \geq R_{\text{NbC}} \qquad \text{[IIc]}$$

where an asterisk indicates the S/L interface, D_L is the liquid diffusivity and $\langle C \rangle_L$ is the intrinsic volume average liquid concentration.

Also, the flux balance at the S/L interface must be satisfied; *i.e.*,

$$V_{\text{NbC}}\,(C^*_{\text{NbC}} - C_L^*) = D_L \left.\frac{\partial C_L}{\partial r}\right|_{r=R^*_{\text{NbC}}} \qquad \text{[IId]}$$

Since the volume fraction of NbC is small at all times, negligible interference between neighboring growing carbides is assumed. Thus, the composition of the bulk liquid should remain effectively $\langle C \rangle_L$. Then, the solutal supersaturation is

$$\Omega_c = \frac{\langle C \rangle_L - C_L^*}{C^*_{\text{NbC}} - C_L^*} \qquad \text{[IIe]}$$

where C_L^*, the liquid interface concentration, is unknown for carbon.

In Reference 5, it was shown (refer also to the tie triangle in Figure 1) that the diffusion path should be such that the interfacial Nb and C concentrations, Nb_L^* and C_L^*, satisfy the following equation, which describes the NbC-γ diffusion couple in alloy 718:

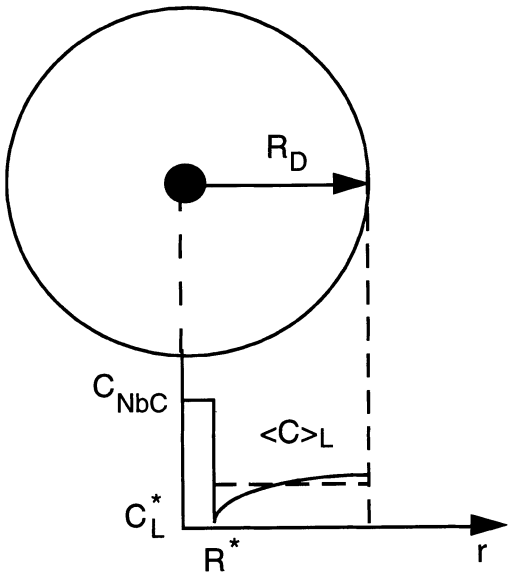

Fig. II—Schematic representation of the diffusion pattern for NbC.

$$D_L^{\text{Nb}} \frac{\partial \text{Nb}(r)}{\partial r} \frac{1}{\text{Nb}_{\text{NbC}} - \text{Nb}_L^*} = D_L^{\text{C}} \frac{\partial C(\text{r})}{\partial r} \frac{1}{C_{\text{NbC}} - C_L^*} \qquad \text{[IIf]}$$

From calculations (refer also to Appendix I),

$$C_{\text{NbC}} >> \langle C \rangle_L >> C_L^* \cong 0 \qquad \text{[IIg]}$$

Also, the concentration gradient can be approximated as (Figure 11a)

$$\left.\frac{\partial C_L}{\partial r}\right|_{r=R_{\text{NbC}}} = \frac{\langle C_L \rangle - C_L^*}{R_D - R_{\text{NbC}}} \qquad \text{[IIh]}$$

Thus, when combining Eqs. [11d] through [h], the growth velocity of the niobium carbide is obtained as

$$V_{\text{NbC}} = \Omega_c \frac{D_L}{R_D - R_{\text{NbC}}} \qquad \text{[IIi]}$$

REFERENCES

1. H.L. Eiselstein: *Advances in the Technology of Stainless Steels and Related Alloys*, ASTM STP, ASTM, Philadelphia, PA, 1965, pp. 62-79.
2. M.J. Cieslak, G.A. Knorovsky, T.J. Headley, and A.D. Roming, Jr.: in *Superalloys 718—Metallurgy and Applications*, E.A. Loria, ed., TMS, Warrendale, PA, 1989, pp. 59-68.
3. R.G. Carlson and J.F. Radavich: in *Superalloys 718—Metallurgy and Applications*, E.A. Loria, ed., TMS, Warrendale, PA, 1989, pp. 79-95.
4. M.J. Cieslak, T.J. Headley, G.A. Knorovsky, A.D. Roming, Jr., and T. Kollie: *Metall. Trans. A*, 1990, vol. 21A, pp. 479-88.
5. B. Radhakrishnan and R.G. Thompson: *Metall. Trans. A*, 1991, vol. 22A, pp. 887-902.
6. C. Chen, R.G. Thompson, and D.W. Davis: in *Superalloys 718, 625 and Various Derivatives*, E.A. Loria, ed., TMS, Warrendale, PA, 1991, pp. 81-96.
7. C. Peyroutou and Y. Honnorat: in *Superalloys 718, 625 and Various Derivatives*, E.A. Loria, ed., TMS, Warrendale, PA, 1991, pp. 309-24.
8. W.D. Cao, R.L. Kennedy, and M.P. Willis: in *Superalloys 718, 625 and Various Derivatives*, E.A. Loria, ed., TMS, Warrendale, PA, pp. 147-60.
9. D. Shangguan, S. Ahuja, and D.M. Stefanescu: *Metall. Trans. A*, 1992, vol. 23A, pp. 669-80.

10. T. Rosenqvist: *Principles of Extractive Metallurgy*, 2nd ed., McGraw-Hill, New York, NY, 1983.
11. H.B. Aaron, D. Fainstein, and G.R. Kotler: *J. Appl. Phys.*, 1970, vol. 41 (11), pp. 4405-09.
12. A.G. Guy, V. Leroy, and T.B. Lindemer: *Trans. ASM*, 1966, vol. 59, pp. 517-34.
13. A.G. Guy and C.B. Smith: *Trans. ASM*, 1962, vol. 55, pp. 1-8.
14. L. Nastac and D.M. Stefanescu: *Metall. Trans. A*, 1993, vol. 24A, pp. 2107-18.
15. L. Nastac and D.M. Stefanescu: *Metall. Mater. Trans. A*, 1997, vol. 28A, pp. 0000-00.
16. L. Nastac: Ph.D. Dissertation, The University of Alabama, Tuscaloosa, AL, 1995.
17. L. Nastac and D.M. Stefanescu: *AFS Trans.*, 1996, in press.
18. D.M. Stefanescu, G. Upadhya, and D. Bandyopadhyay: *Metall. Trans. A*, 1990, vol. 21A, pp. 997-1005.
19. Y.K. Ko and J.T. Berry: NASA CASTNET Review and ICCA Task Team Meeting, Auburn University, Auburn, AL, May 1994, pp. 31-42.